

Supplementary Information

An Acid–Base Responsive Supramolecular Drawstring with Switchable Fluorescence

Xiangyu Dong^a, Liang-Liang Mao^a, Zhaoming Zhang^b, Zi-Tong Li^a, Sheng-Nan Lei^a, Xuzhou Yan^b, Chen-Ho Tung^a, Li-Zhu Wu^a, Huan Cong^{a*}

^a Key Laboratory of Photochemical Conversion and Optoelectronic Materials, CAS-HKU Joint Laboratory on New Materials, Technical Institute of Physics and Chemistry; School of Future Technology, University of Chinese Academy of Sciences, Chinese Academy of Sciences, 100190, Beijing, China,

^b State Key Laboratory of Synergistic Chem-Bio Synthesis, Frontiers Science Center for Transformative Molecules, School of Chemistry and Chemical Engineering, Shanghai Jiao Tong University, 200240, Shanghai, China

* Corresponding Author: Huan Cong
E-mail: hcong@mail.ipc.ac.cn

Table of Contents

Page S2: **I. General Information**

Page S3: **II. Synthetic Procedures and Compound Characterization**

Page S11: **III. Host–Guest Assembly Characterization**

Page S14: **IV. Photophysical Properties**

Page S17: **V. Acid–Base Responsive Properties**

Page S20: **VI. Supramolecular Drawstring-Incorporated Polymer**

Page S24: **VII. Preparation of PABHN-Loaded Paper**

Page S25: **VIII. References**

I. General Information

NMR spectra were recorded with a Bruker Avance 400 or Ascend 600 spectrometer at 25 °C, and were internally referenced to residual protio solvent signals (for example, CDCl_3 was referenced at 7.26 and 77.16 ppm, respectively).^{S1} Data for ^1H NMR were reported as follows: chemical shift (δ ppm), integration, multiplicity (br = broad, ovrlp = overlapping, s = singlet, d = doublet, t = triplet, q = quartet, m = multiplet), and coupling constant (Hz) when applicable. All ^{13}C NMR spectra were recorded with complete proton decoupling. Infrared spectra were recorded on a Varian 3100 FT-IR or a Bruker Tensor 27 spectrometer. DOSY experiments were recorded with a Bruker Avance 600 spectrometer. High-resolution mass spectrometry experiments were performed with a Bruker Daltonics Apex IV spectrometer. UV-Vis spectra of liquid samples were recorded in 1 cm quartz cuvette using a Varian Cary 5000 UV-Vis spectrometer. The absolute singlet quantum yield, emission lifetime, and fluorescence spectra of liquid and solid samples were measured using an Edinburgh FLS1000 or FLSP920 spectrometer. The mechanical properties of the polymers were measured using an Instron 3343 machine for standard stress–strain experiments.

All reactions were carried out using flame-dried glassware under nitrogen atmosphere unless otherwise noted. Analytical thin layer chromatography (TLC) was performed using 0.25 mm silica gel 60-F plates. Flash chromatography was performed using 200–400 mesh silica gel. HPLC-grade tetrahydrofuran, dichloromethane, toluene, and hexanes were purified and dried by passing through a PURE SOLV® solvent purification system (Innovative Technology, Inc.). Deionized water was degassed by bubbling with a nitrogen balloon for 20 min prior to use as reaction solvent. Chemical reagents were purchased from Energy Chemicals, Heowns, Innochem, and J&K, and were used as received.

II. Synthetic Procedures and Compound Characterization

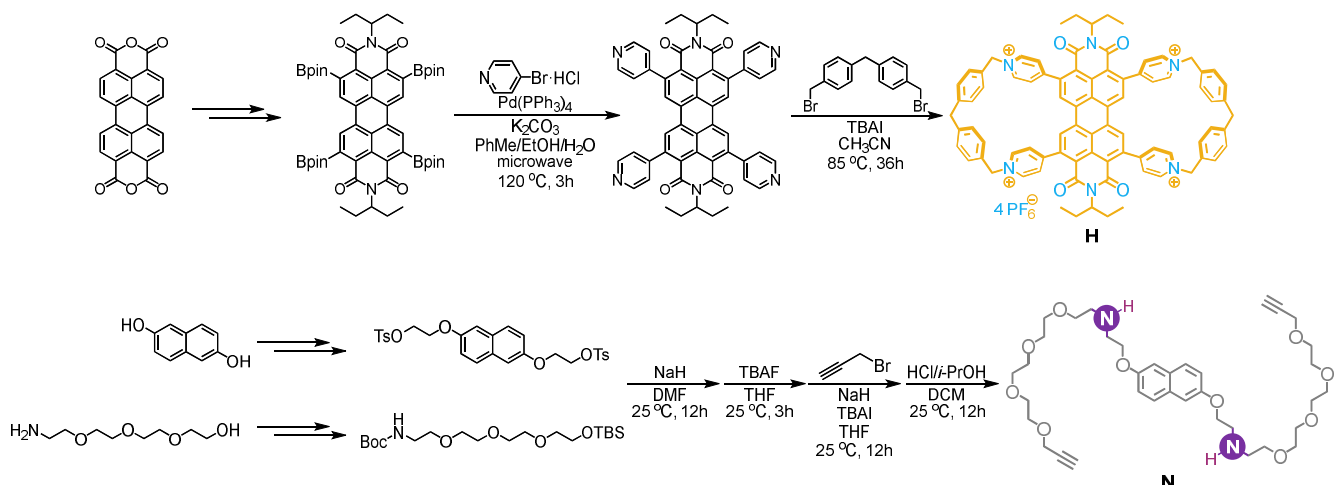
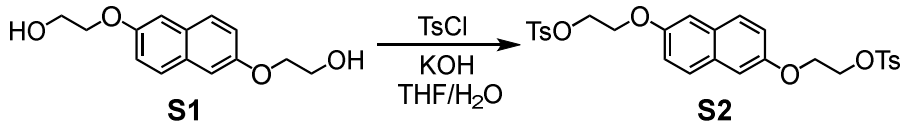


Figure S1. Synthetic routes of **H** and **N**.



In air, compound **S1** (4.22 g, 17 mmol, 1.0 equiv., prepared according to the literature^{S2}) and THF (20 mL) were added to a 250 mL round-bottom flask equipped with a stir bar. The solution was stirred at 0 °C for 10 minutes, before the addition of a stock solution of KOH (5.86 g, 102 mmol, 6.0 equiv.) in H₂O (20 mL) at 0 °C. After stirred at 25 °C for 30 minutes, a stock solution of *p*-toluenesulfonyl chloride (7.05 g, 37 mmol, 2.2 equiv.) in THF (20 mL) was added into the flask. After stirred at 25 °C for 12 hours, reaction mixture was concentrated under reduced pressure, and H₂O was added to the flask. The precipitate was collected by filtering, sequentially washed with H₂O and ethanol, and air-dried. Compound **S2** (7.63 g, 80% yield) was obtained as a white solid.

Compound **S2**

¹H NMR (400 MHz, CD₃CN) δ 7.80 (d, *J* = 8.4 Hz, 4H), 7.62 (d, *J* = 9.2 Hz, 2H), 7.40 (d, *J* = 8.0 Hz, 4H), 7.10 (d, *J* = 2.4 Hz, 2H), 6.99 (dd, *J* = 9.2, 2.4 Hz, 2H), 4.40–4.36 (m, 4H), 4.25–4.21 (m, 4H), 2.40 (s, 6H);
¹³C NMR (101 MHz, CDCl₃) δ 154.8, 145.1, 133.1, 130.0, 129.9, 128.4, 128.2, 119.2, 107.4, 68.3, 65.7, 21.8;
IR (KBr): 1603, 1370, 1358, 1238, 1188, 1177, 966, 930, 775 cm⁻¹;
HRMS (ESI): [M+Na]⁺ calcd for [C₂₈H₂₈O₈S₂Na]⁺ 579.1118, found 579.1127.

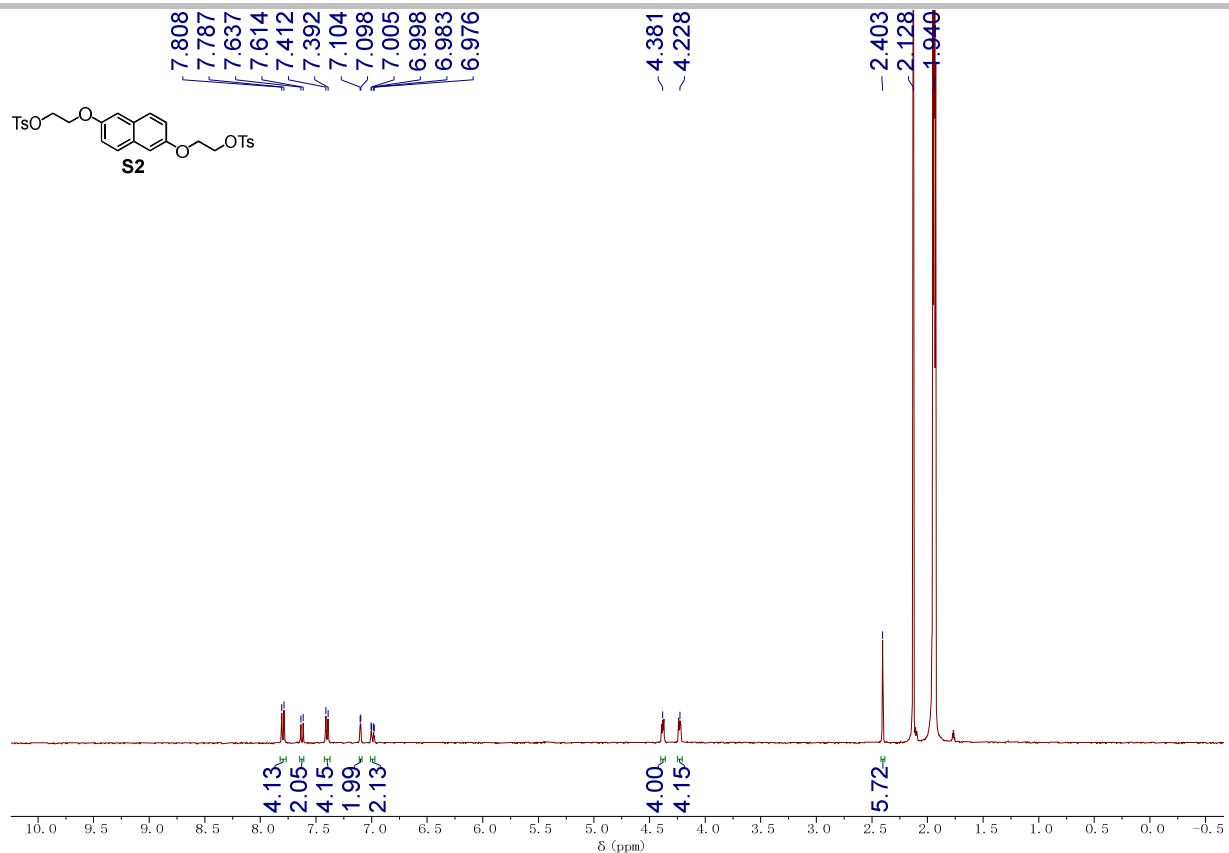


Figure S2. ^1H NMR spectrum (CD_3CN , 400 MHz, 298 K) of **S2**.

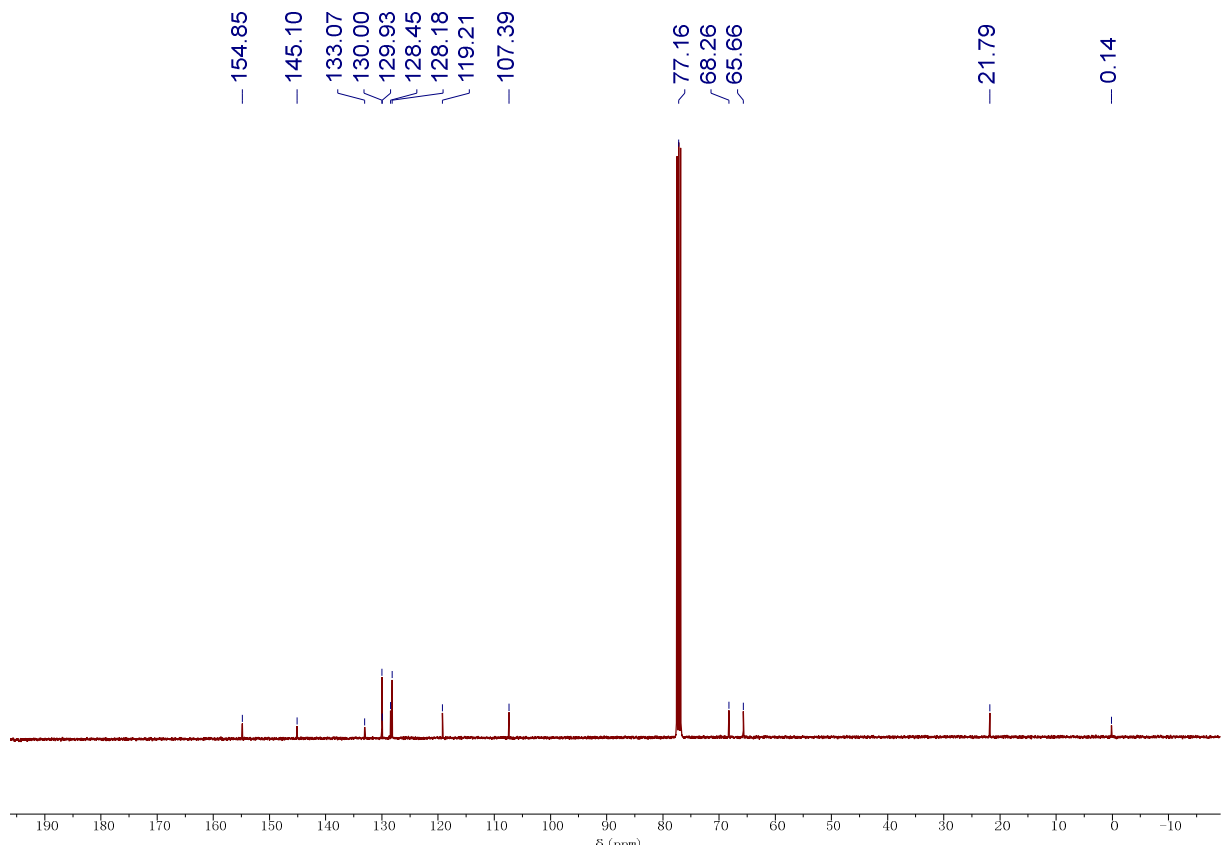
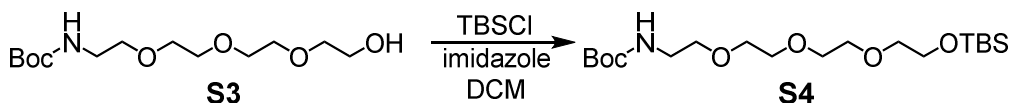


Figure S3. ^{13}C NMR spectrum (CDCl_3 , 101 MHz, 298 K) of **S2**.



In air, compound **S3** (2.43 g, 8.3 mmol, 1.0 equiv., prepared according to the literature^{S3}), imidazole (1.36 g, 20 mmol, 2.4 equiv.) and anhydrous CH₂Cl₂ (10 mL) were added to a 40 mL glass vial equipped with a stir bar. After the solution was stirred at 25 °C for 10 minutes, a stock solution of tert-butyldimethylsilyl chloride (1.51 g, 10 mmol, 1.2 equiv.) in CH₂Cl₂ (10 mL) was added into the vial. After stirred at 25 °C for 3 hours, reaction mixture was concentrated under reduced pressure. The residue was mixed with H₂O and extracted with ethyl acetate. The organic layer was washed with brine, and dried using anhydrous sodium sulfate. The solvents were removed under reduced pressure. Purification using silica gel column chromatography (petroleum ether: ethyl acetate = 4:1) afforded compound **S4** (3.22 g, 95% yield) as colorless oil.

Compound S4

¹H NMR (400 MHz, CD₃CN) δ 5.32 (s, 1H), 3.75–3.70 (m, 2H), 3.58–3.52 (m, 8H), 3.51–3.47 (m, 2H), 3.47–3.42 (m, 2H), 3.17 (p, *J* = 5.6 Hz, 2H), 1.40 (s, 9H), 0.89 (s, 9H), 0.06 (s, 6H);

¹³C NMR (101 MHz, CD₃CN) δ 156.8, 79.2, 73.4, 71.3, 71.2, 71.1, 70.9, 70.6, 63.6, 41.0, 28.6, 26.3, 19.0, -5.0;

IR (KBr): 3365, 2931, 1717, 1520, 1473, 1391, 1366, 1006, 941 cm^{-1} ;

HRMS (ESI): $[M+Na]^+$ calcd for $[C_{19}H_{41}O_6NSiNa]^+$ 430.2595, found 430.2603.

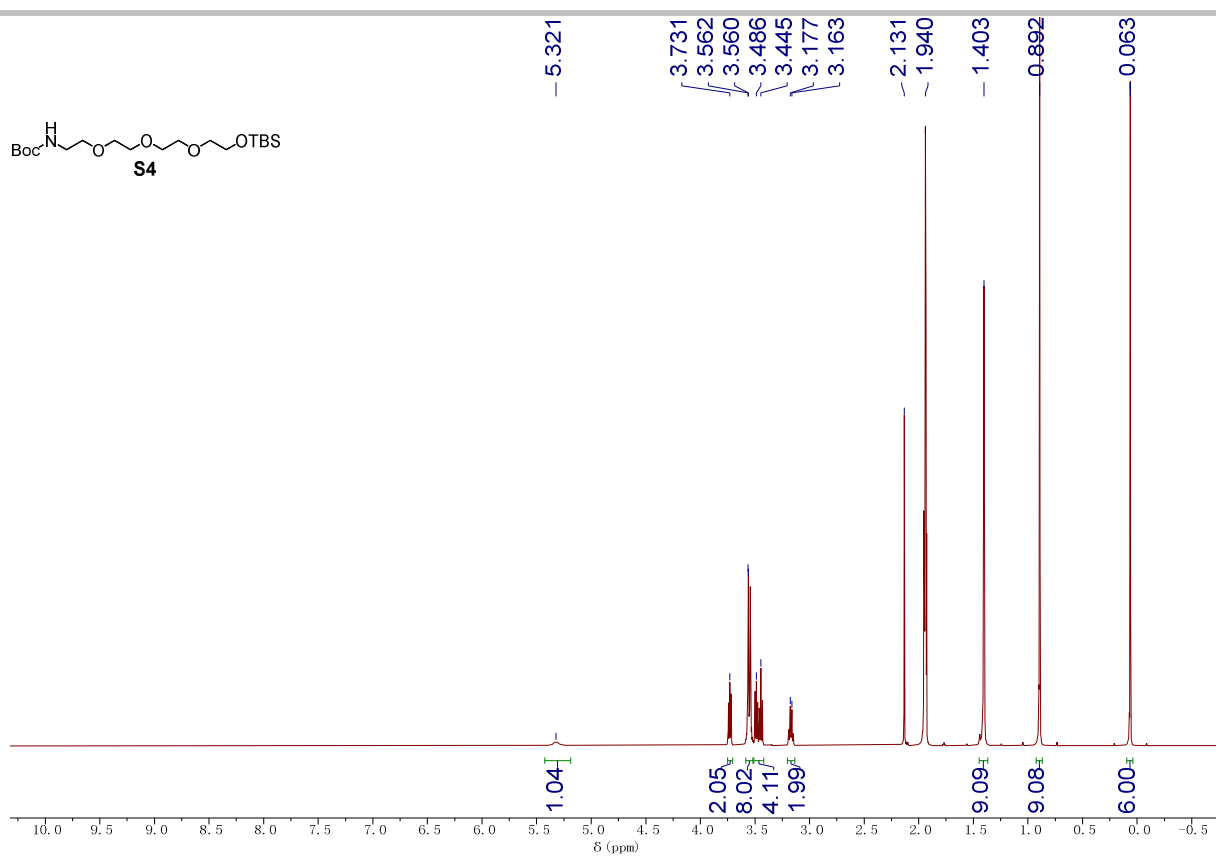


Figure S4. ^1H NMR spectrum (CD_3CN , 400 MHz, 298 K) of **S4**.

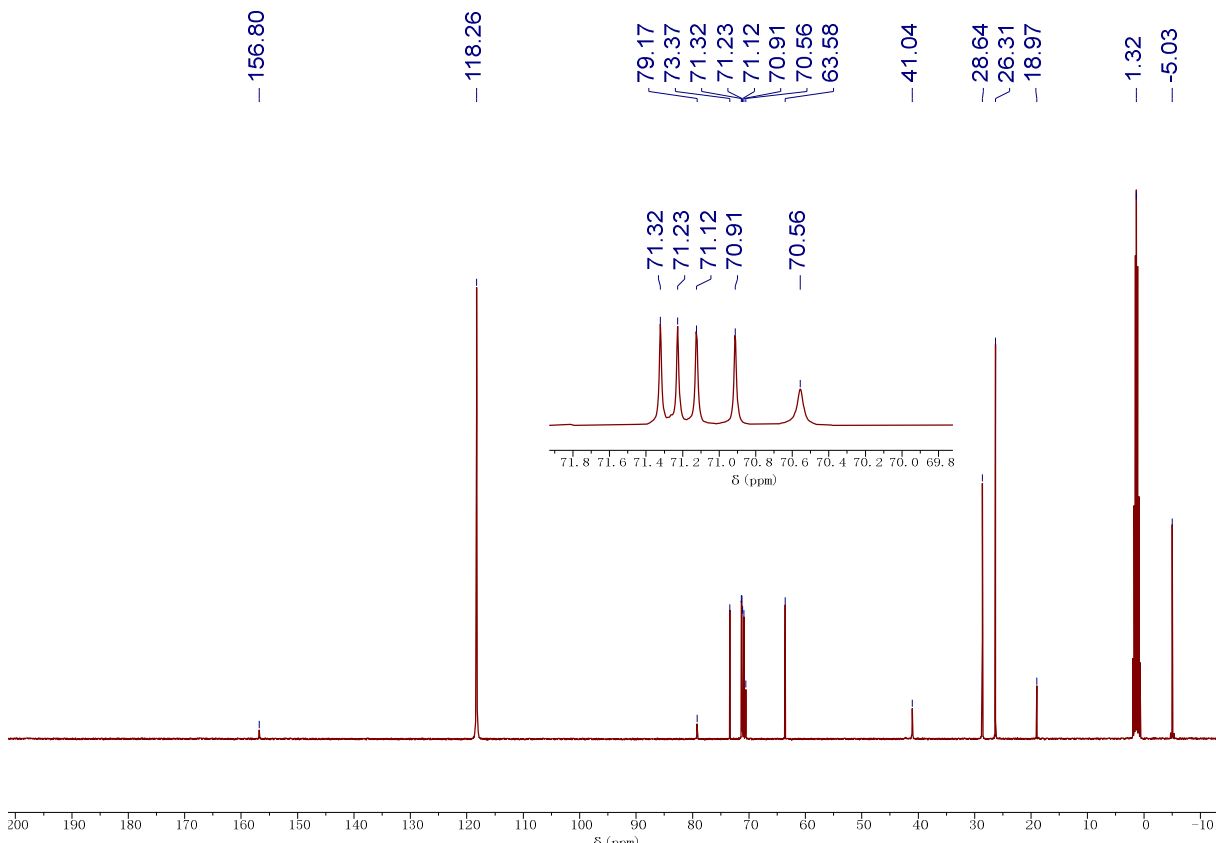
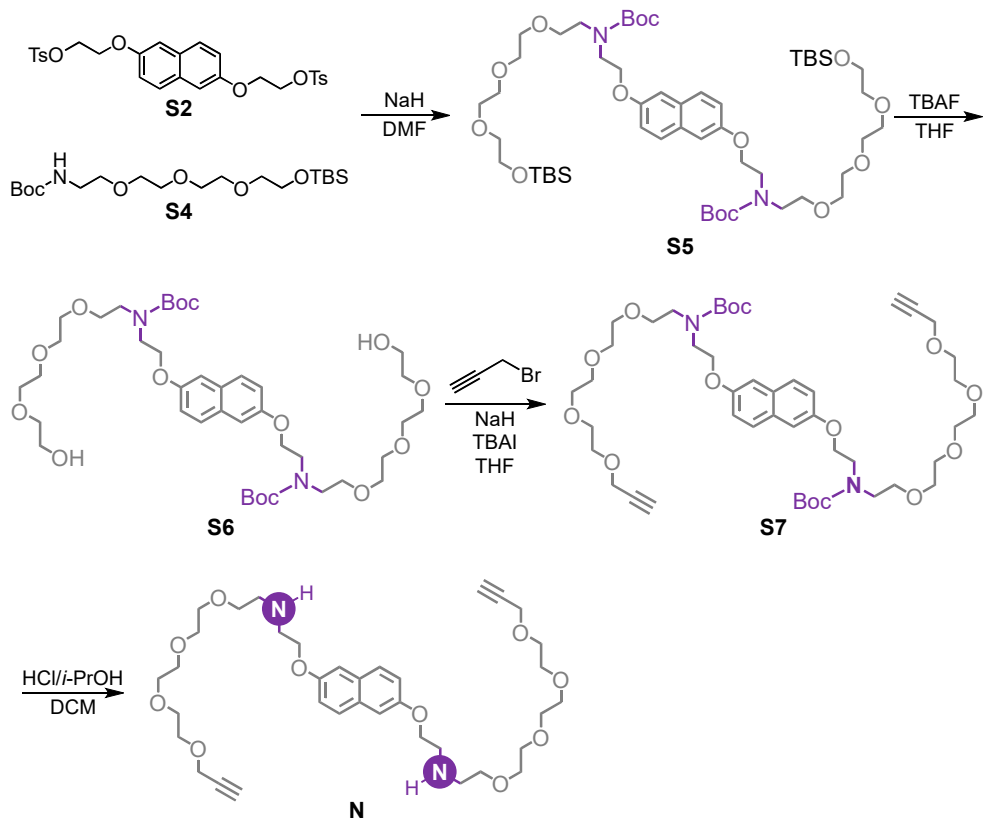


Figure S5. ^{13}C NMR spectrum (CD_3CN , 101 MHz, 298 K) of **S4**.



Step 1:

In air, compound **S4** (2.45 g, 6.0 mmol, 3.0 equiv.) and anhydrous DMF (4 mL) were added to a 40 mL glass vial equipped with a stir bar. The solution was stirred at 0 °C for 5 minutes, before the addition of a stock solution of NaH (60% dispersion in mineral oil, 192 mg, 8.0 mmol, 4.0 equiv.) in DMF (2 mL) at 0 °C. After the solution was stirred at 0 °C for 30 minutes, a suspension of compound **S2** (1.11 g, 2.0 mmol, 1.0 equiv.) in DMF (2 mL) was added into the vial at 0 °C. After stirred at 25 °C for 12 hours, the reaction mixture was diluted with H₂O and extracted with ethyl acetate. The combined organic layers were washed with brine, and dried using anhydrous sodium sulfate. The solvents were removed under reduced pressure and filtrated through a short silica column with the aid of mixed (petroleum ether: ethyl acetate = 7:3). The solvents were removed under reduced pressure, affording the crude compound **S5** which was used in the next step without further purification.

Step 2:

In air, crude **S5** from *Step 1* and anhydrous THF (4 mL) were added to a 40 mL glass vial equipped with a stir bar. The solution was stirred at 0 °C for 5 minutes, before the addition of a stock solution of TBAF (497 mg, 1.9 mmol) in THF (1.9 mL) at 0 °C. After stirred at 25 °C for 3 hours, the reaction mixture was diluted with H₂O and extracted with ethyl acetate. The combined organic layers were washed with brine, and dried using anhydrous sodium sulfate. The solvents were removed under reduced pressure and filtrated through a short silica column with the aid of mixed (CH₂Cl₂: CH₃OH = 25:2). The solvents were removed under reduced pressure, affording the crude compound **S6** which was used in the next step without further purification.

Step 3:

In air, NaH (60% dispersion in mineral oil, 60 mg, 2.5 mmol) and anhydrous THF (4 mL) were added to a 40 mL glass vial equipped with a stir bar. The solution was stirred at 0 °C for 5 minutes, before the addition of a stock solution of crude **S6** from *Step 2* in THF (4 mL) at 0 °C. After the solution was stirred at 0 °C for 20 minutes, TBAI (31 mg, 0.084 mmol) and 3-bromopropyne (297 mg, 2.5 mmol) was added into the vial at 0 °C. After stirred at 25 °C for 12 hours, the reaction mixture was diluted with H₂O and extracted with ethyl acetate. The combined organic layers were washed with brine, and dried using anhydrous sodium sulfate. The solvents were removed under reduced pressure and filtrated through a short silica column with the aid of mixed (CH₂Cl₂: CH₃OH = 100:3). The solvents were removed under reduced pressure, affording the crude compound **S7** which was used in the next step without further purification.

Step 4:

In air, crude **S7** from *Step 3*, and anhydrous CH₂Cl₂ (4 mL) were added to a 40 mL glass vial equipped with a stir bar, and the resulting solution was stirred at 0 °C for 5 minutes before the addition of HCl (2.0 M in ethanol, 1.8 mL, 3.7 mmol) at 0 °C. After stirred at 25 °C for 12 hours, the reaction mixture was diluted with H₂O and extracted with CH₂Cl₂. The combined organic layers were washed with saturated NaHCO₃ aqueous solution (40 mL × 3) and brine, and dried using anhydrous sodium sulfate. The solvents were removed under reduced pressure, affording compound **N** (399 mg, 30% yield for four step) as brown oil.

Compound N:

¹H NMR (400 MHz, CD₃CN) δ 7.68 (d, *J* = 9.2 Hz, 2H), 7.22 (d, *J* = 2.8 Hz, 2H), 7.12 (dd, *J* = 9.2, 2.8 Hz, 2H), 4.17–4.08 (m, 8H), 3.64–3.42 (m, 28H), 3.07–2.97 (m, 4H), 2.86–2.77 (m, 4H), 2.69 (t, *J* = 2.4 Hz, 2H);

¹³C NMR (101 MHz, CD₃CN) δ 156.4, 130.8, 129.1, 120.0, 108.1, 80.9, 75.7, 71.3, 71.2 (br), 71.0, 70.9, 69.9, 68.71, 58.7, 49.9, 49.4;

IR (KBr): 3254, 2870, 2362, 1605, 1509, 1359, 1233, 1116, 852 cm⁻¹;

HRMS (ESI): [M+Na]⁺ calcd for [C₃₆H₅₄O₁₀N₂Na]⁺ 697.3671, found 697.3672.

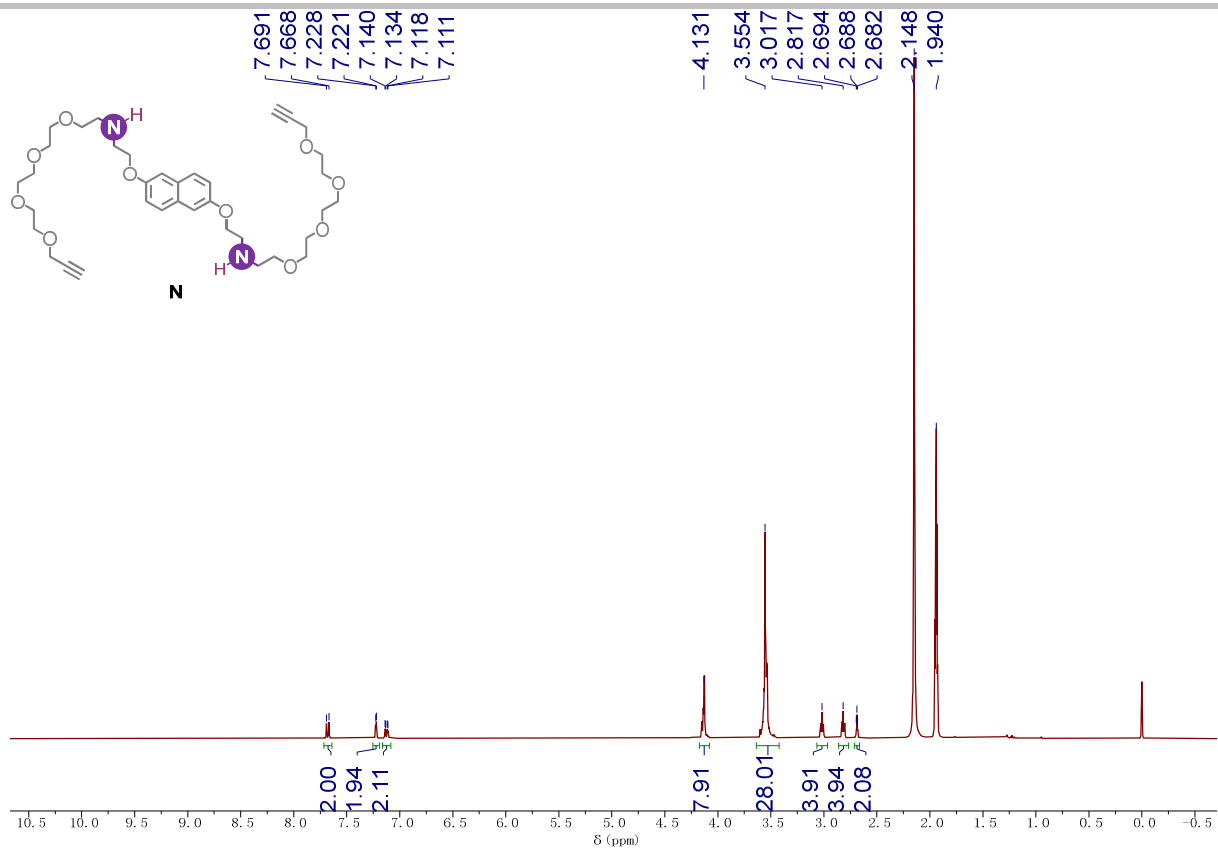


Figure S6. ¹H NMR spectrum (CD₃CN, 400 MHz, 298 K) of **N**.

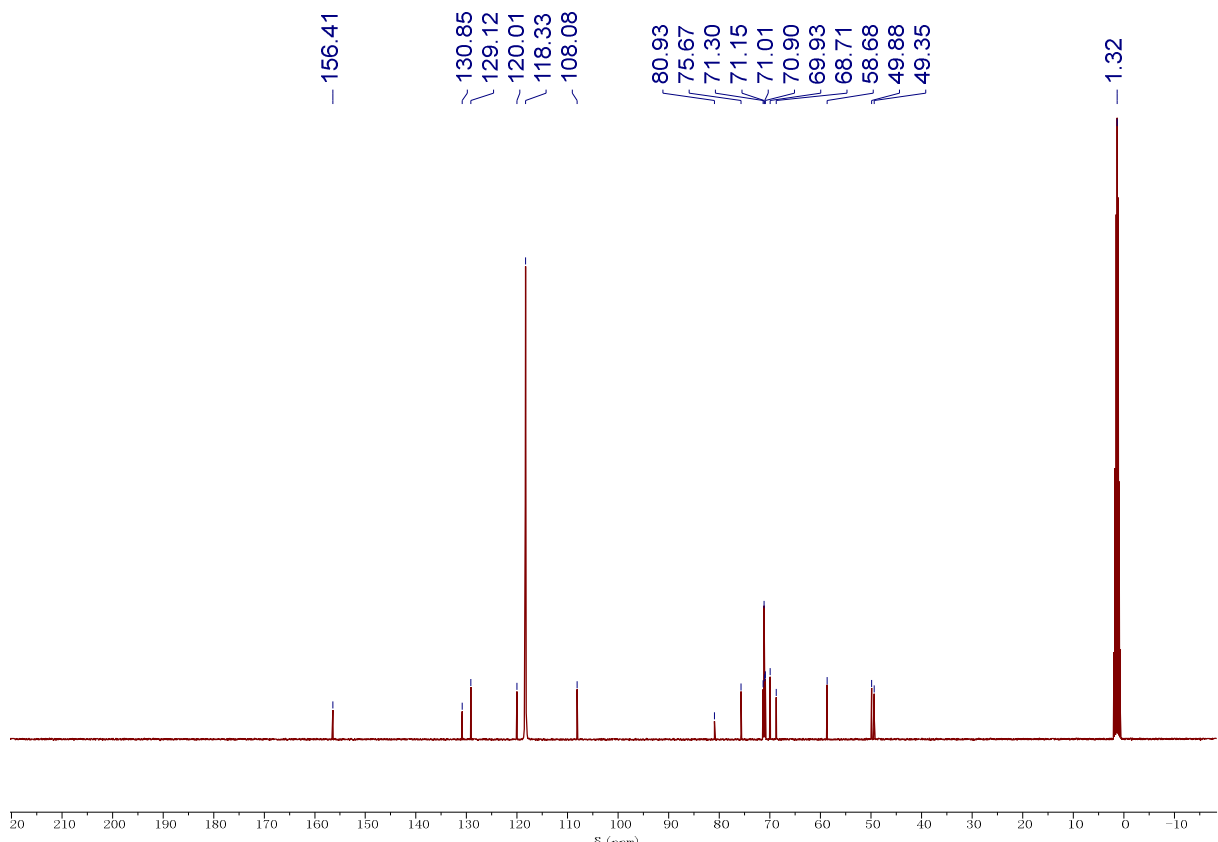
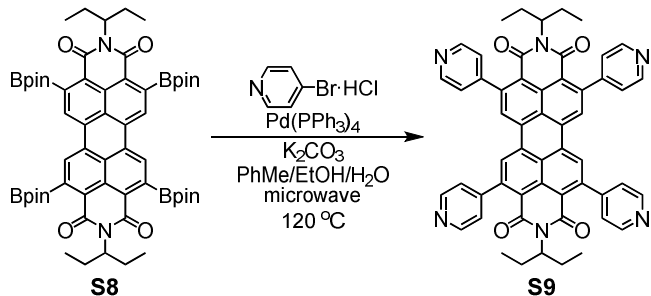


Figure S7. ¹³C NMR spectrum (CD₃CN, 101 MHz, 298 K) of **N**.

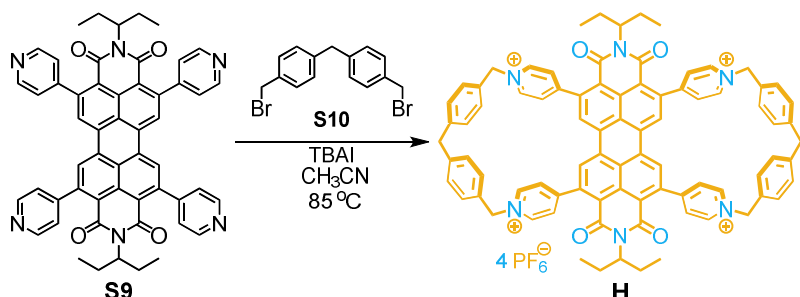


In a nitrogen-filled glove box, compound **S8** (1.03 g, 1.0 mmol, 1.0 equiv., prepared according to the literature^{S4}), 4-bromopyridine hydrochloride (1.56 g, 8.0 mmol, 8.0 equiv.), $\text{Pd}(\text{PPh}_3)_4$ (462 mg, 0.40 mmol, 40 mol%), K_2CO_3 (2.76 g, 20 mmol, 20 equiv.), and toluene (10 mL) were added to a 20 mL microwave reaction vial equipped with a stir bar. The vial was sealed with a Teflon-lined septum cap, and transferred out of glove box. Degassed ethanol (4.0 mL) and degassed H_2O (2.0 mL) were sequentially added to the reaction vial via a syringe. The reaction vial was transferred to the microwave reactor (conditions: 200 W, 120 °C, 3 h). After cooled down to room temperature, the solvents were removed under reduced pressure. The crude product was washed by H_2O (40 mL × 3) and CH_2Cl_2 (30 mL × 3), affording compound **S9** (738 mg, 88% yield) as an orange solid.

Compound **S9**:

(Characterization data are consistent with literature *Angew. Chem. Int. Ed.* **2024**, e202318368.)

^1H NMR (400 MHz, CDCl_3) δ 8.77 (d, J = 6.0 Hz, 8H), 8.30 (s, 4H), 7.33 (d, J = 6.0 Hz, 8H), 4.80–4.74 (m, 2H), 2.05–1.94 (m, 4H), 1.79–1.71 (m, 4H), 0.85 (t, J = 7.4 Hz, 12H).



In a nitrogen-filled glove box, compound **S9** (84 mg, 0.10 mmol, 1.0 equiv.), compound **S10** (71 mg, 0.20 mmol, 2.0 equiv., prepared according to the literature^{S5}), tetrabutylammonium iodide (3.7 mg, 0.010 mmol, 0.10 equiv.) and anhydrous CH_3CN (200 mL) were added to a 500 mL round-bottom flask equipped with a stir bar. The flask was capped and transferred out of glove box. The reaction mixture was stirred and refluxed under nitrogen at 85 °C for 36 h, then cooled to room temperature. The solvents were removed under reduced pressure, and H_2O (400 mL) was added to the flask. After treated with ultrasonic for 10 minutes, the resulting mixture was filtered. The filtrate was mixed with excess NH_4PF_6 (200 mg, 1.2 mmol), and treated with ultrasonic for another 10 minutes. The precipitate was collected by centrifugation, sequentially washed with H_2O and CH_2Cl_2 , and air-dried. Compound **H** (88 mg, 49% yield) was obtained as a red solid.

Compound **H**:

(Characterization data are consistent with literature *Angew. Chem. Int. Ed.* **2024**, e202318368.)

^1H NMR (400 MHz, CD_3CN) δ 8.93 (d, J = 6.0 Hz, 8H), 8.21 (s, 4H), 7.97 (d, J = 6.0 Hz, 8H), 7.52 (d, J = 8.0 Hz, 8H), 7.44 (d, J = 7.6 Hz, 8H), 5.75 (s, 8H), 4.69–4.59 (m, 2H), 4.02 (s, 4H), 1.92–1.67 (m, 8H), 0.81 (t, J = 7.4 Hz, 12H).

III. Host–Guest Assembly Characterization

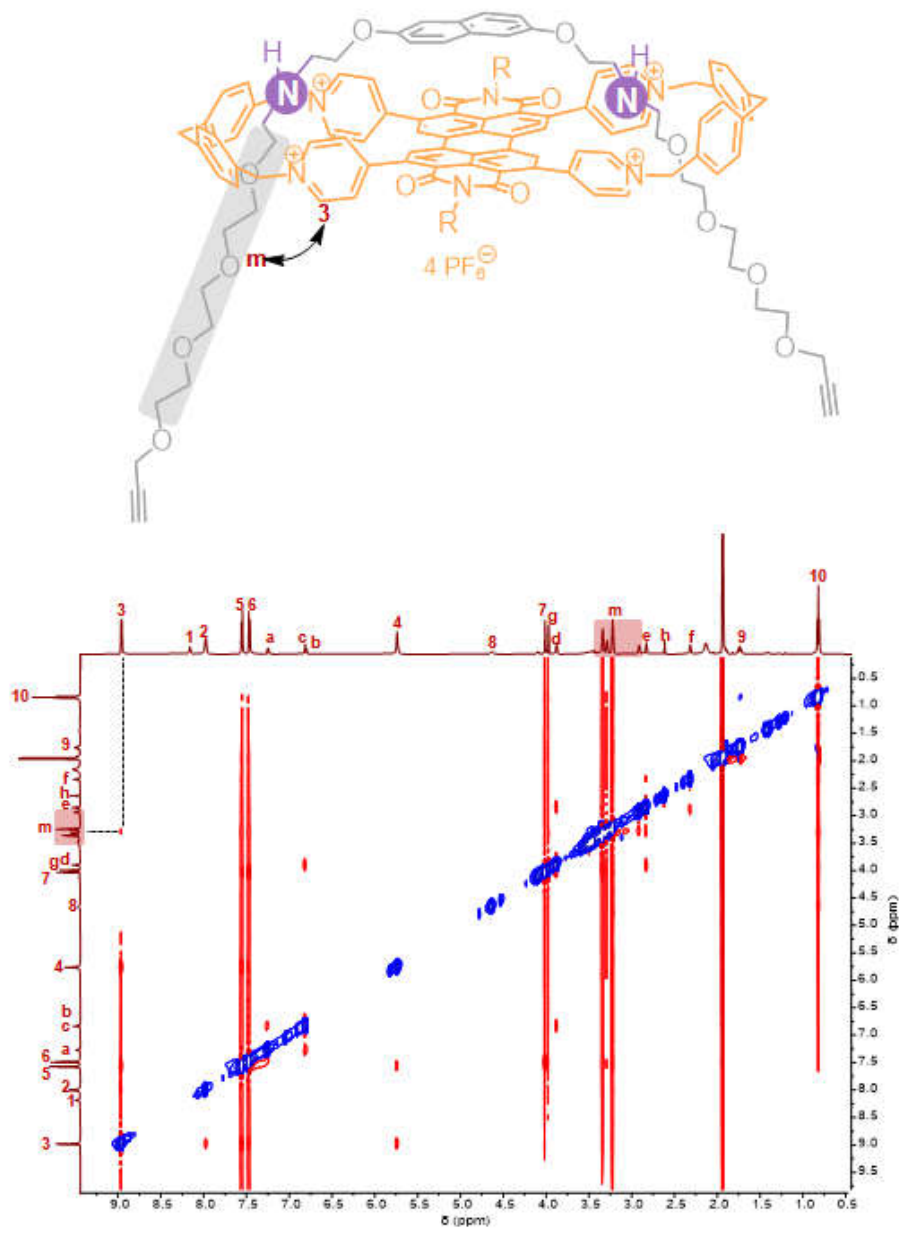


Figure S8. ROESY spectrum (CD_3CN , 600 MHz, 298 K) of **H–N** complex.

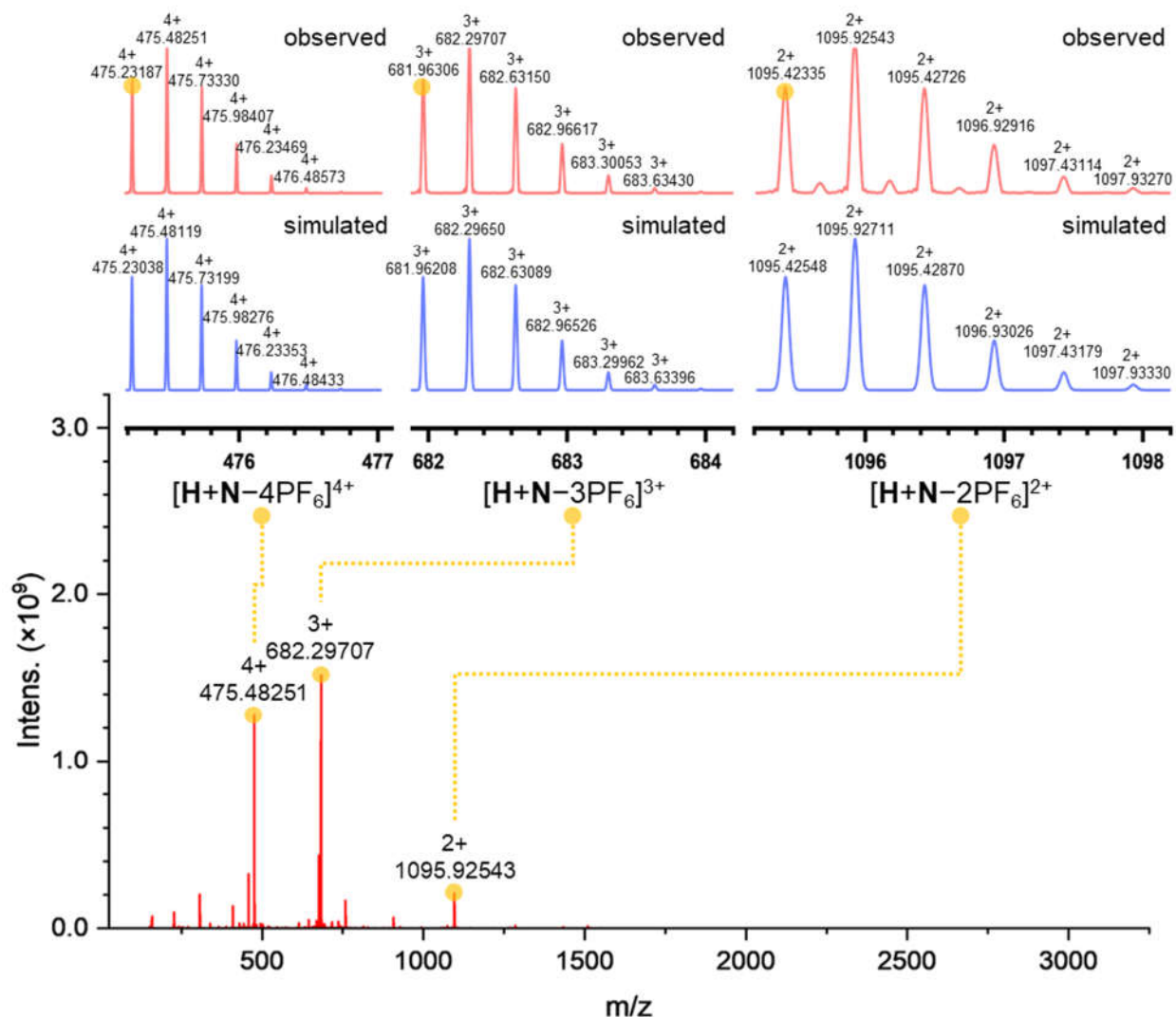


Figure S9. The HR-MS data of an acetonitrile solution containing **H** and **N** (1:1 molar ratio).

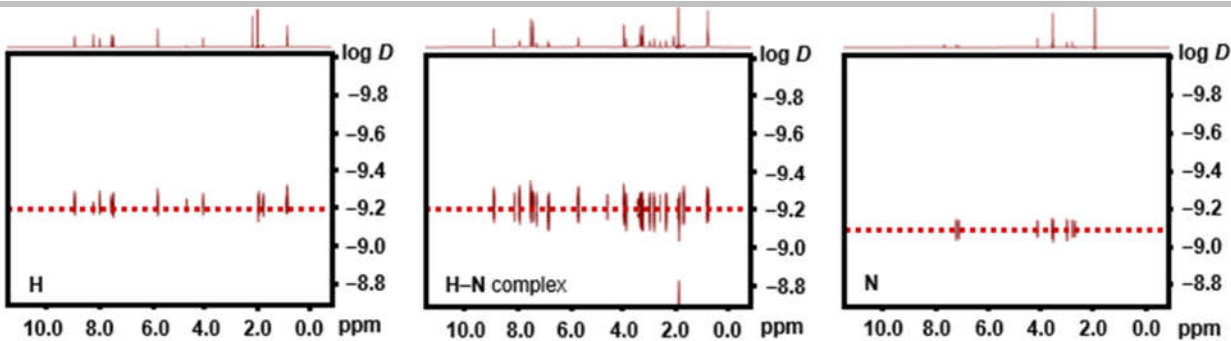


Figure S10. DOSY spectrum (CD₃CN, 600 MHz, 298 K) of **H**, **H–N** complex (1:1 molar ratio of **H** and **N**) and **N**.

The hydrodynamic radii of **H**, **H–N** complex and **N** were calculated from the DOSY data according to the literature.^{S6}

Assuming that the diffusing entity is a sphere, according to Stokes–Einstein equation,

$$D = \frac{k_B T}{6\pi\eta r_h(sp)}$$

Where D is the molecule's diffusion coefficient (measured by DOSY experiments), k_B is the Boltzmann constant, T is the experimental temperature (298 K), $r_h(sp)$ is the molecule's hydrodynamic radius using the spherical model, and η is the viscosity of the solvent (for CD₃CN at 298 K, 0.000334 Pa·s).^{S7} Based on the above, the calculated hydrodynamic radius r_h for **H**, **H–N** complex, and **N** were summarized in **Table S1**. The size parameters derived from the DOSY data are consistent with the desired structures.

Table S1. Summary of size parameters of **H**, **H–N** complex, and **N** derived from DOSY data

	H	H–N complex	N
log D	-9.201	-9.201	-9.071
D (m ² ·s ⁻¹)	6.3×10 ⁻¹⁰	6.3×10 ⁻¹⁰	8.5×10 ⁻¹⁰
k_B (N·m·K ⁻¹)		1.38×10 ⁻²³	
T (K)		298	
η (Pa·s)		3.34×10 ⁻⁴	
$r_h(sp)$ (nm)	1.0	1.0	0.77

IV. Photophysical Properties

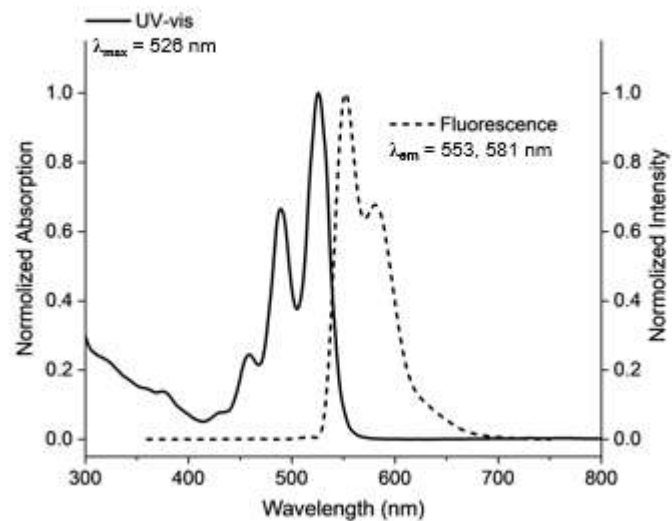


Figure S11. UV-Vis and fluorescence ($\lambda_{\text{ex}} = 340 \text{ nm}$) spectra of H ($5 \times 10^{-5} \text{ M}$ in CH_3CN) at 25°C .

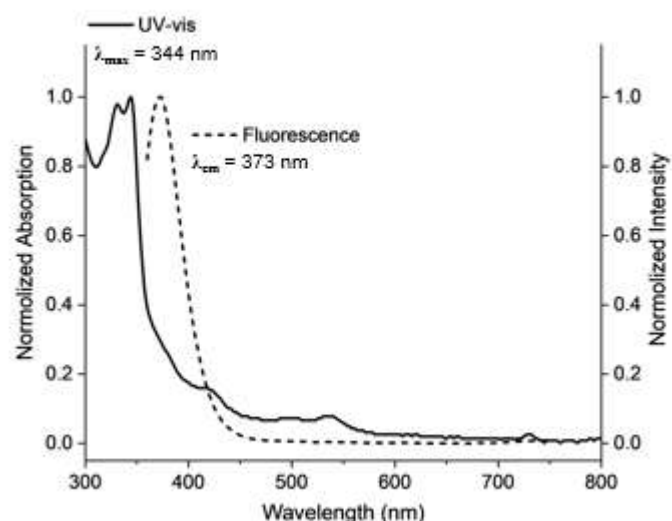


Figure S12. UV-Vis and fluorescence ($\lambda_{\text{ex}} = 340 \text{ nm}$) spectra of N ($5 \times 10^{-5} \text{ M}$ in CH_3CN) at 25°C .

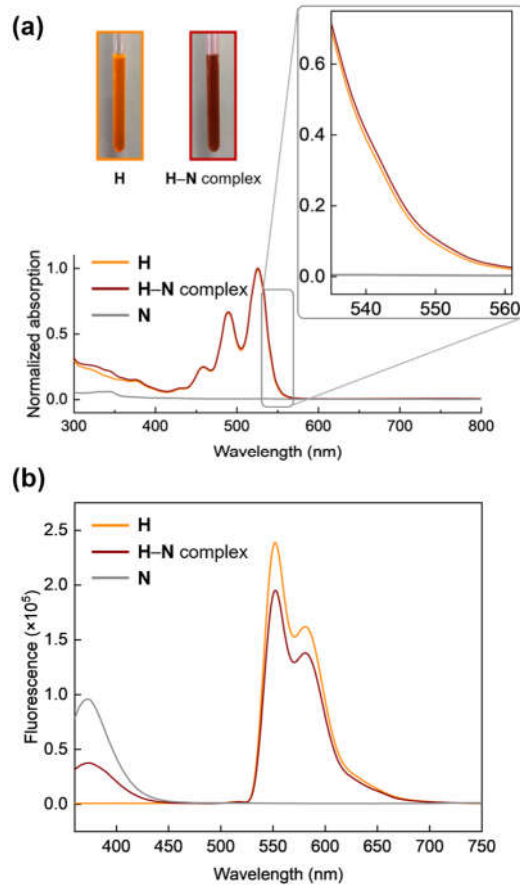


Figure S13. (a) UV-Vis and (b) fluorescence ($\lambda_{\text{ex}} = 340$ nm) spectra of **H** (5×10^{-5} M), **N** (5×10^{-5} M), and **H**-**N** complex (1:1 molar ratio of **H** and **N**, 5×10^{-5} M each) in CH_3CN at 25°C . Inset: photographs of **H** (2.5×10^{-3} M) and **H**-**N** complex (1:1 molar ratio of **H** and **N**, 2.5×10^{-3} M each).

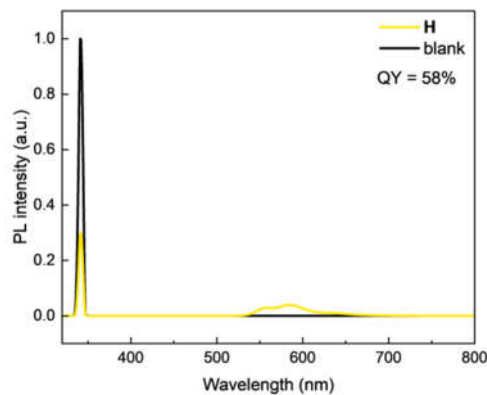


Figure S14. Quantum yield of **H** in CH_3CN at 25°C .

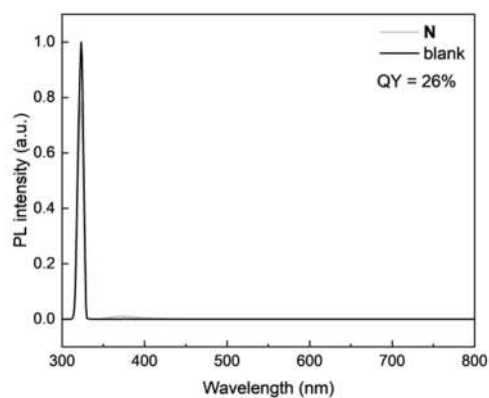


Figure S15. Quantum yield of **N** in CH_3CN at 25°C .

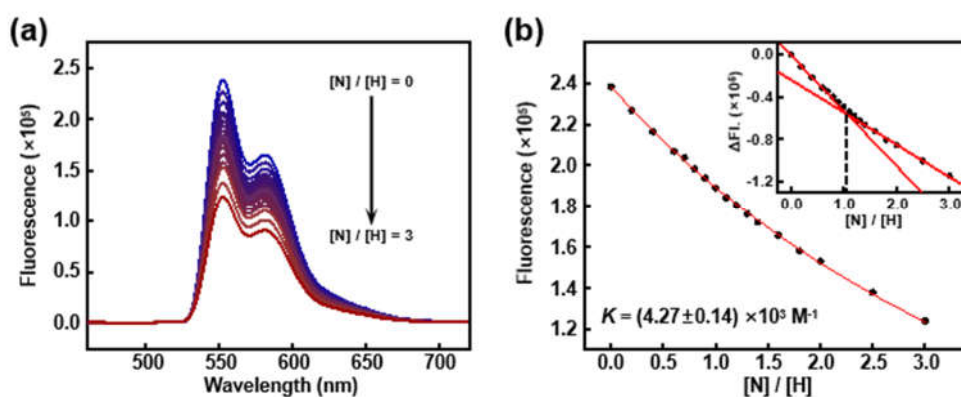


Figure S16. (a) Fluorescence titration of **H** (5×10^{-5} M in CH_3CN , with excitation wavelength of 340 nm) with **N** at 25°C . (b) Binding constant of **H**–**N** complex. (Inset) Mole ratio plot indicating a 1:1 stoichiometry.

V. Acid–Base Responsive Properties

N +5 eq. TFA

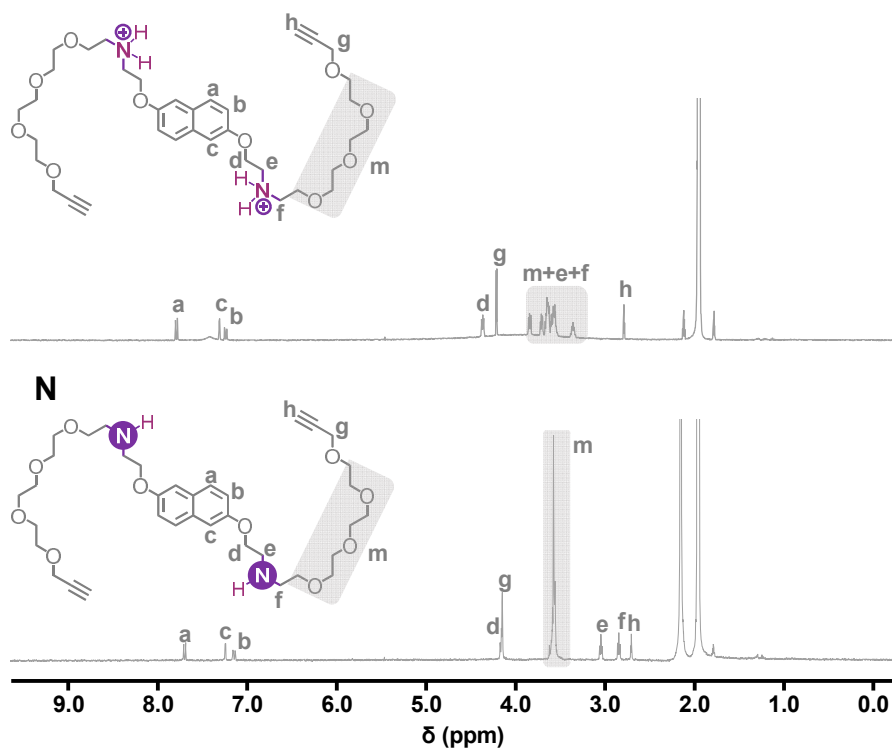
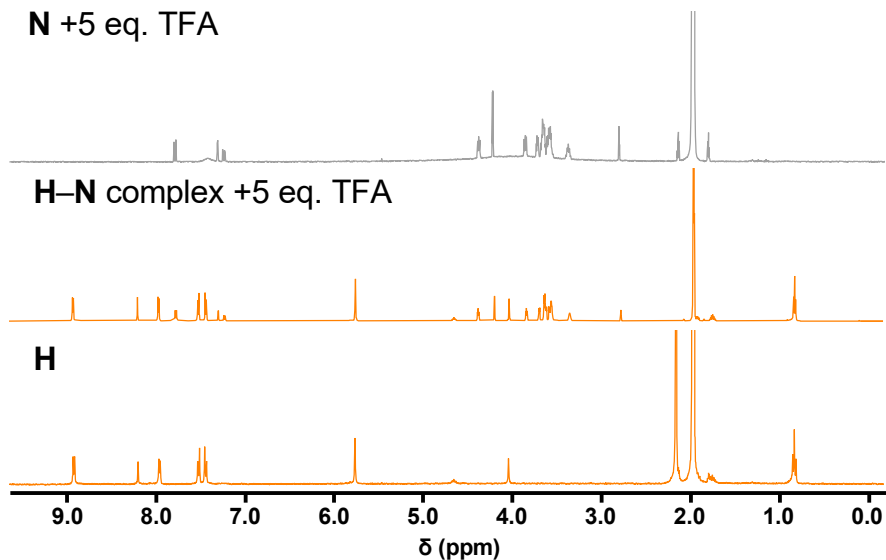


Figure S17. ¹H NMR spectra (CD₃CN, 400 MHz, 298 K) of **N** before and after TFA (5 equiv.) addition.

N +5 eq. TFA



H–N complex +5 eq. TFA

H

Figure S18. ¹H NMR spectra (CD₃CN, 400 MHz, 298 K) of **N** and **H–N** complex in the presence of TFA (5 equiv.), in comparison with **H**.

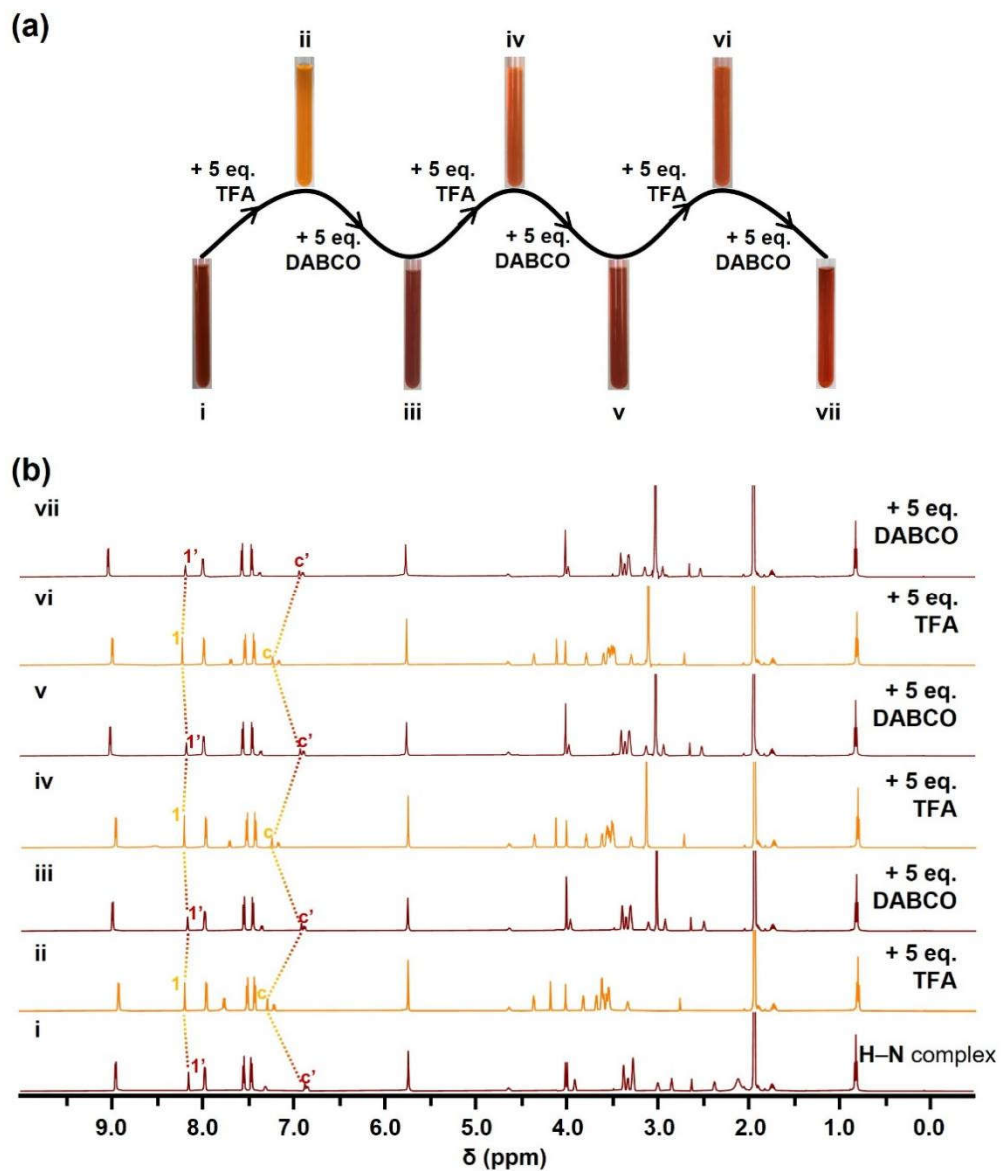


Figure S19. (a) Photographs and (b) ^1H NMR spectra (600 MHz, 298 K) of (i) **H–N** complex (2.5×10^{-3} M in CD_3CN) and (ii–vii) after sequential addition of TFA and DABCO.

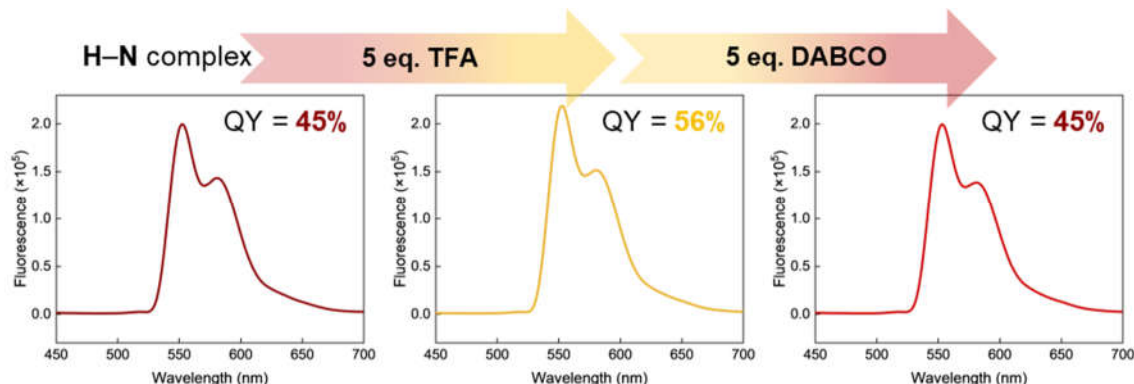


Figure S20. Fluorescence spectra ($\lambda_{\text{ex}} = 340$ nm, in CH_3CN , 25 °C) and quantum yield of **H–N** complex (1:1 molar ratio of **H** and **N**, 5×10^{-5} M each) in response to the sequential addition of TFA and DABCO.

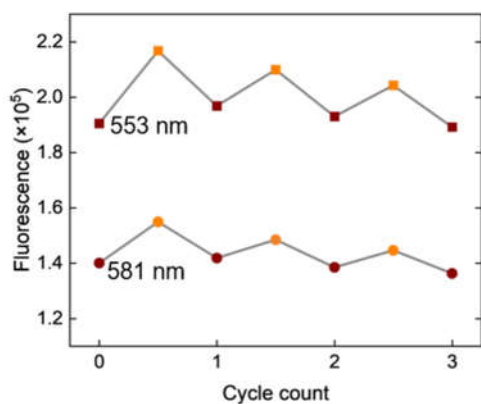


Figure S21. The changes in the fluorescence intensity of **H–N** complex (1:1 molar ratio of **H** and **N**, 5×10^{-5} M each) following sequential addition with TFA (orange data points) and DABCO (brown data points).

VI. Supramolecular Drawstring-Incorporated Polymer

Preparation of supramolecular drawstring-incorporated polymer **PABHN**

In air, compound **A1** (311 mg, 0.99 mmol), **A2** (47 mg, 0.20 mmol), **B** (375 mg, 1.3 mmol), triethylamine (5.0 mg, 0.050 mmol), and $\text{Cu}(\text{CH}_3\text{CN})_4\text{PF}_6$ (2.4 mg, 0.0065 mmol) were dissolved in a mixture composed of **N** (6.7 mg, 0.010 mmol), **H** (9.0 mg, 0.0050 mmol) and CH_3CN (1 mL) at room temperature. The reaction vial was sealed with a Teflon-lined cap. After treated with ultrasonic for 5 minutes, the viscous mixture was poured into a Teflon mold ($40 \times 15 \times 4$ mm) and air-dried at 25°C for 12 h, affording the polymer samples as dark red film. Finally, the polymer film of **PABHN** was rinsed with CH_3CN and air-dried.

Preparation of polymer **PAB** (control group)

In air, compound **A1** (314 mg, 1.0 mmol), **A2** (47 mg, 0.20 mmol), **B** (375 mg, 1.3 mmol), triethylamine (5.0 mg, 0.050 mmol), and $\text{Cu}(\text{CH}_3\text{CN})_4\text{PF}_6$ (2.4 mg, 0.0065 mmol) were dissolved in CH_3CN (1 mL) at room temperature. The reaction vial was sealed with a Teflon-lined cap. After treated with ultrasonic for 5 minutes, the viscous mixture was poured into a Teflon mold ($40 \times 15 \times 4$ mm) and air dried at 25°C for 12 h, affording the polymer samples as yellow film. Finally, the polymer film of **PAB** was rinsed with CH_3CN and air-dried.

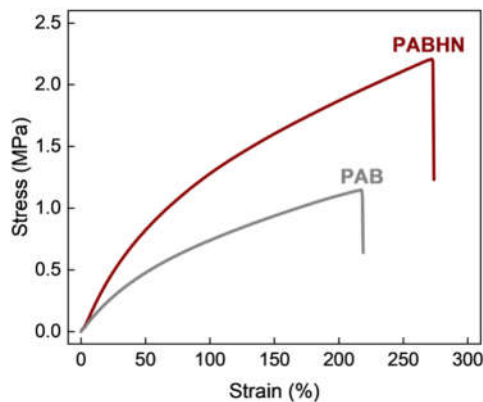


Figure S22. Stress-strain curves of **PABHN** and **PAB** recorded at 25°C with a deformation rate of 100 mm/min.

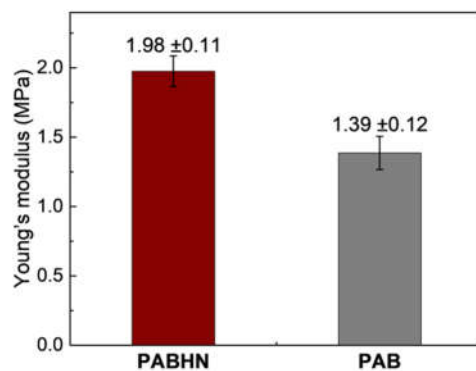


Figure S23. Young's modulus of **PABHN** and **PAB** based on their stress–strain curves.

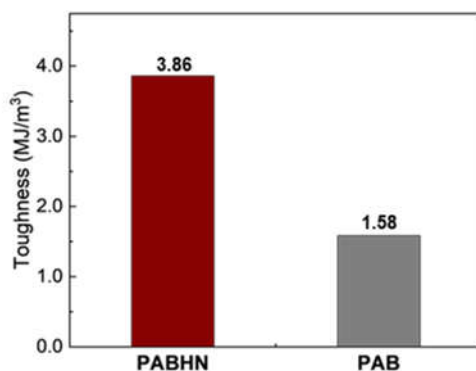


Figure S24. Toughness of **PABHN** and **PAB** based on their stress–strain curves.

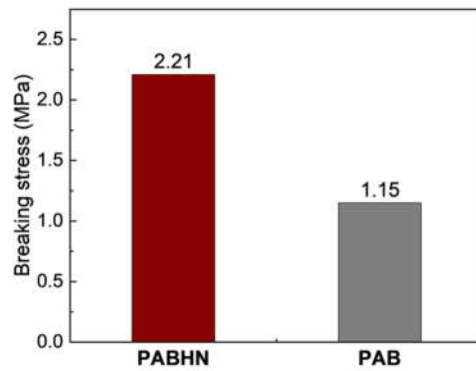


Figure S25. Breaking stress of **PABHN** and **PAB** based on their stress–strain curves.

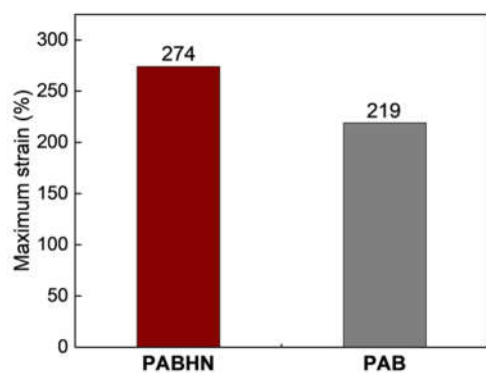


Figure S26. Maximum strain of **PABHN** and **PAB** based on their stress–strain curves.

Preparation of supramolecular drawstring-integrated polymer **PABHN** (acidic form)

The **PABHN** sample was soaked in 0.5% (v/v) solution of TFA in acetonitrile for 1 hour at room temperature. Then it was soaked and rinsed with fresh acetonitrile (200 mL). The soak–rinse cycle was repeated for three times. After air-dried, the sample **PABHN** (acidic form) was obtained.

Preparation of supramolecular drawstring-integrated polymer **PABHN** (neutralized form)

The **PABHN** (acidic form) sample was soaked in 0.5% (v/v) solution of diethylamine (DEA) in acetonitrile for 1 hour at room temperature. Then it was soaked and rinsed with fresh acetonitrile (200 mL). The soak–rinse cycle was repeated for three times. After air-dried, the sample **PABHN** (neutralized form) was obtained.

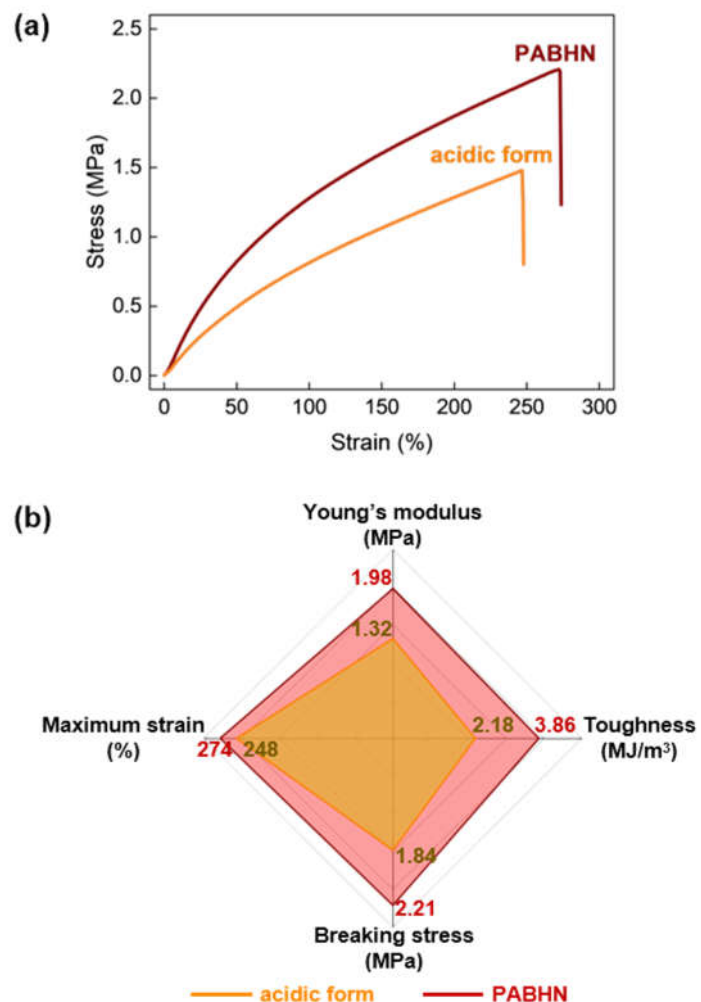


Figure S27. (a) Stress–strain curves of **PABHN** and **PABHN** (acidic form) recorded at 25 °C with a deformation rate of 100 mm/min. (b) Comparison of mechanical properties of **PABHN** and **PABHN** (acidic form).

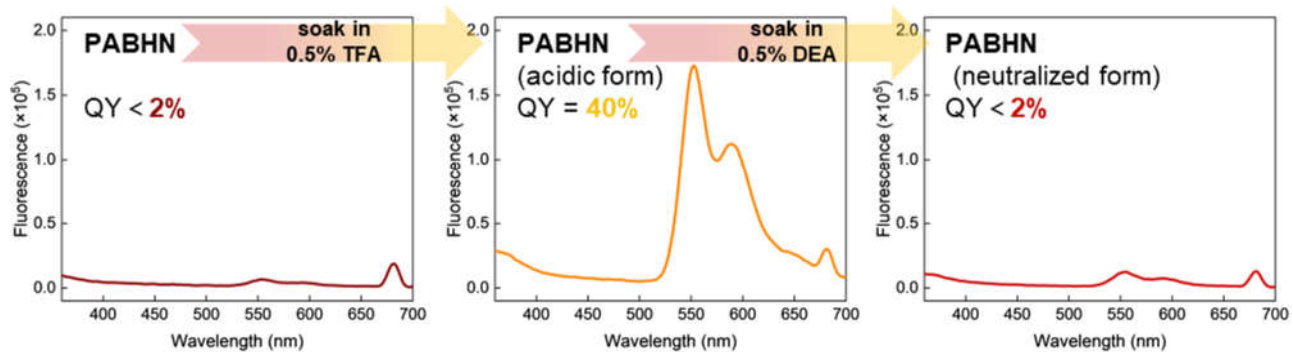


Figure S28. Fluorescence spectra ($\lambda_{\text{ex}} = 340$ nm, 25 °C) and quantum yield of **PABHN** films in response to the sequential treatment of TFA and DEA. The peak at 650-700 nm is the second harmonic peak.

VII. Preparation of PABHN-Loaded Paper

A piece of filter paper (4 cm × 5 cm) was placed in a stainless-steel tray. The stock solution for synthesizing **PABHN** was added onto the filter paper dropwise, which contains **A1** (311 mg, 0.99 mmol), **A2** (47 mg, 0.20 mmol), **B** (375 mg, 1.3 mmol), **N** (6.7 mg, 0.010 mmol), **H** (9.0 mg, 0.0050 mmol), triethylamine (5.0 mg, 0.050 mmol), Cu(CH₃CN)₄PF₆ (2.4 mg, 0.0065 mmol), and CH₃CN (1.0 mL). The filter paper which fully absorbed the stock solution was exposed to open air and kept at 25 °C for 12 hours. Subsequently, the filter paper was rinsed with fresh acetonitrile and air-dried to obtain the **PABHN**-loaded paper.

pH-Responsive fluorescence property of PABHN loaded paper (Figure 5c)

A piece of PABHN-loaded paper was covered with a stainless steel mask (with hollow patterns) and sprayed with a 0.5% solution of TFA in acetonitrile. This produced the pattern with yellow fluorescence. Then, the paper was immersed in a 0.5% solution of DEA in acetonitrile for 30 minutes, making the pattern to fade completely. After drying, the paper was covered with another mask (with different hollow patterns) and sprayed with freshly squeezed lemon juice, generating the new fluorescent pattern.

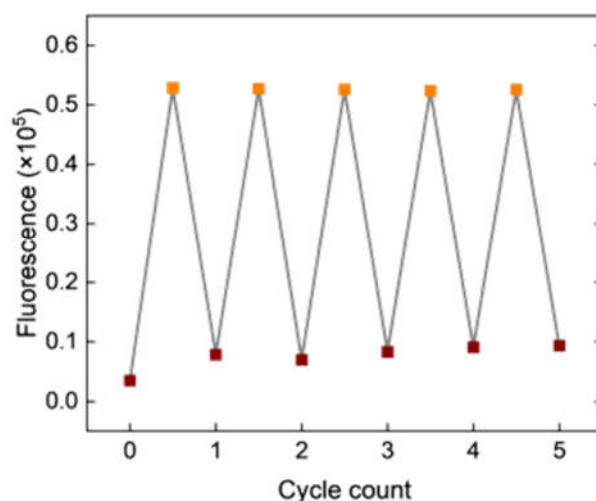


Figure S29. Reversible switching for the fluorescence intensity ($\lambda_{\text{em}} = 553$ nm) of **PABHN**-loaded paper following 5 cycles of sequential treatment of TFA (orange data points) and DEA (brown data points).

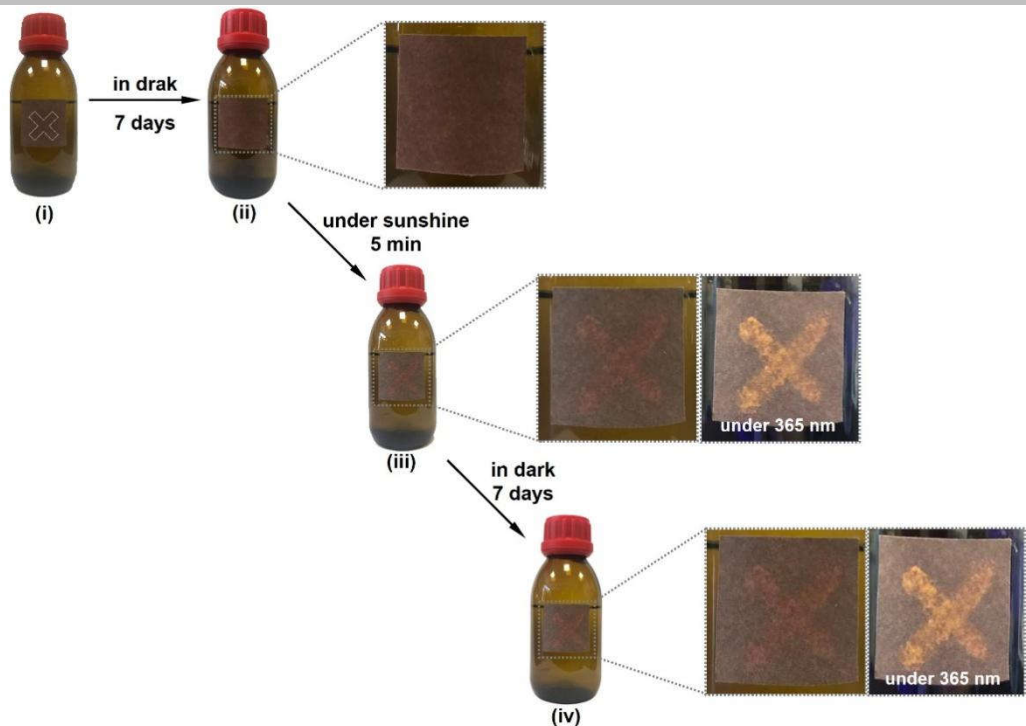


Figure S30. Photographs of security labels for monitoring light-exposure history.

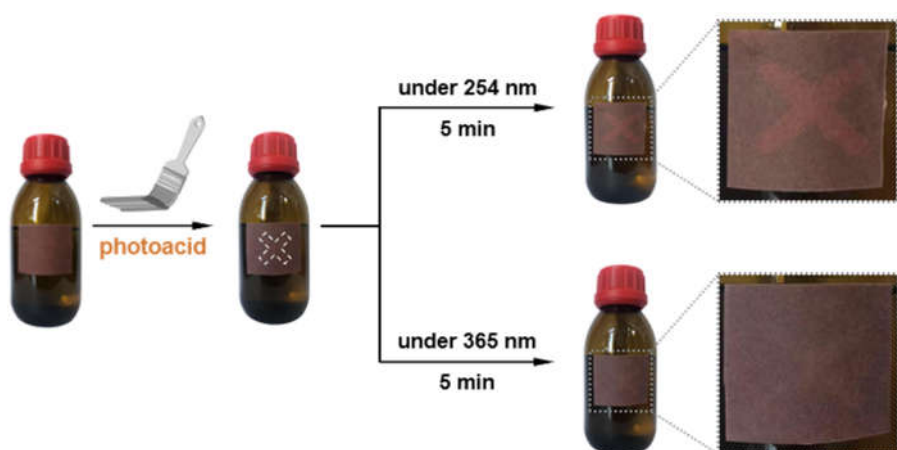


Figure S31. Photographs of security labels showing the response to 254 nm and 365 nm UV irradiation at 25 °C.

Note: The results showed fast fluorescence turn-on under 254 nm, but not under 365 nm.

VIII. References

[S1] G. R. Fulmer, A. J. M. Miller, N. H. Sherden, H. E. Gottlieb, A. Nudelman, B. M. Stoltz, J. E. Bercaw and K. I. Goldberg, NMR Chemical Shifts of Trace Impurities: Common Laboratory Solvents, Organics, and Gases in Deuterated Solvents Relevant to the Organometallic Chemist, *Organometallics*, 2010, **29**, 2176–2179.

[S2] S.-C. Kao, Y.-C. Lin, I. Ryu and Y.-K. Wu, Revisiting Hydroxyalkylation of Phenols with Cyclic Carbonates, *Adv. Synth. Catal.*, 2019, **361**, 3639.

[S3] L. Jierry, N. Ben Ameur, J.-S. Thomann, B. Frisch, E. Gonthier, J.-C. Voegel, B. Senger, G. Decher, O. Felix, P. Schaaf, P. Mesini and F. Boulmedais, Influence of Cu(I)–Alkyne π -Complex Charge on the Step-by-Step Film Buildup through Sharpless Click Reaction, *Macromolecules*, 2010, **43**, 3994–3997.

[S4] F. S. Conrad-Burton, T. Liu, F. Geyer, R. Costantini, A. P. Schlaus, M. S. Spencer, J. Wang, R. H. Sánchez, B. Zhang, Q. Xu, M. L. Steigerwald, S. Xiao, H. Li, C. P. Nuckolls and X. Zhu, Controlling Singlet Fission by Molecular Contortion, *J. Am. Chem. Soc.*, 2019, **141**, 13143–13147.

[S5] K.-Y. Peng, S.-A. Chen and W.-S. Fann, Efficient Light Harvesting by Sequential Energy Transfer across Aggregates in Polymers of Finite Conjugational Segments with Short Aliphatic Linkages, *J. Am. Chem. Soc.*, 2001, **123**, 11388–11397.

[S6] B. M. Schulze, D. L. Watkins, J. Zhang, I. Ghiviriga and R. K. Castellano, Estimating the Shape and Size of Supramolecular Assemblies by Variable Temperature Diffusion Ordered Spectroscopy, *Org. Biomol. Chem.*, 2014, **12**, 7932–7936.

[S7] D. R. Lide, W. M. Haynes, G. Baysinger, L. I. Berger, M. Frenkel, R. N. Goldberg, H. V. Kehiaian, K. Kuchitsu, K. Roth and D. Zwillinger, *CRC Handbook of Chemistry and Physics, 90th Edition (CD-ROM Version 2010)*.